Modeling CO2 Capture in Amine Solvents: Prediction of Performance and Insights on Limiting Phenomena

ARTICLE *in* INDUSTRIAL & ENGINEERING CHEMISTRY RESEARCH · MARCH 2013

Impact Factor: 2.59 · DOI: 10.1021/ie302768s

4 AUTHORS:

Thibaut Neveux
Électricité de France (EDF)
15 PUBLICATIONS **57** CITATIONS
SEE PROFILE

Yann Le Moullec
Électricité de France (EDF)
40 PUBLICATIONS **345** CITATIONS
SEE PROFILE

Jean-Pierre Corriou
University of Lorraine
130 PUBLICATIONS **1,271** CITATIONS
SEE PROFILE

Eric Favre
French National Centre for Scientific Research
137 PUBLICATIONS **1,822** CITATIONS
SEE PROFILE

I&EC research
Industrial & Engineering Chemistry Research

Article

pubs.acs.org/IECR

Modeling CO_2 Capture in Amine Solvents: Prediction of Performance and Insights on Limiting Phenomena

Thibaut Neveux,[†,‡] Yann Le Moullec,[†] Jean-Pierre Corriou,[§,‡] and Eric Favre*[,§,‡]

[†]Department of Fluid Dynamics, Power Generation and Environment, EDF R&D, 6 quai Watier, F-78400 Chatou, France
[‡]Laboratoire Réactions et Génie des Procédés LRGP, Université de Lorraine, UPR 3349, ENSIC, F-54000 Nancy, France
[§]Laboratoire Réactions et Génie des Procédés LRGP, CNRS, UPR 3349, ENSIC, F-54000 Nancy, France

ABSTRACT: A model of absorption and stripping columns is developed for post-combustion CO_2 capture in amine solvents. The model is based on a rigorous thermodynamic framework, the extended UNIQUAC model, for the representation of vapor−liquid equilibria (VLE) in order to characterize different solvents in a wide range of concentration and temperature. A rate-based formulation of chemically enhanced heat and mass transfer is used for the packed column model. Two modeling approaches are used for mass transfer in film: an enhancement factor model and a diffusion-reaction model. The rigorous absorption and stripping models have been successfully validated against experimental results from an industrial and a laboratory pilot plant. A sensitivity analysis is performed in order to emphasize the role of limiting phenomena on the separation performance, which concludes that none of the phenomena can be neglected. The interfacial area is the most sensitive parameter on absorber performance, whereas the heat of desorption is the prevailing parameter in the stripper. The CO_2 equilibrium constant is a sensitive parameter in both absorption and stripping units. The two film models are compared and give similar results for the monoethanolamine solvent. However, the comparison must be redone for each implemented solvent since physicochemical properties are modified, e.g., reaction kinetics, diffusion coefficients, and VLE constants. New insights are given on the contribution of CO_2 and H_2O on heat fluxes between phases for the absorber and the stripper. Especially, water condensation and evaporation along the packing impact directly the CO_2 removal efficiency and reboiler heat duty.

1. INTRODUCTION

CO_2 capture in power plants is a suitable option to reduce atmospheric emissions of power plants and to achieve world emissions targets.[1] Post-combustion CO_2 capture is a short-term to medium-term solution, particularly adapted for power plant retrofitting. Among post-combustion processes, chemical absorption in an amine solvent is the most developed process. However, its implementation in the power plant requires a steam drawoff from the power plant steam cycle, which induces a power plant efficiency loss of 10%−12% without advanced integration, including CO_2 compression.[2]

In order to reduce this efficiency loss, many academic and industrial studies focus either on the formulation and characterization of new promising solvents[3,4] or on the improvement of integrated flow schemes.[5,6] Nevertheless, these approaches should be coupled, because the optimal flow scheme depends on the solvent due to its particular physicochemical properties, e.g., kinetics of absorption, cyclic capacity, heat of regeneration, and temperature of thermal degradation.

A simplified process flow diagram of a typical CO_2 capture process by chemical absorption is presented in Figure 1. Such a process is mainly composed of three sections: an absorber where CO_2 is separated from the flue gas exiting the power plant by absorption in an alkanolamine aqueous solution, a stripper where the solvent is regenerated by heat provided in a reboiler, and an economizer where the sensible heat between the CO_2 lean hot stream and the CO_2-rich cold stream is exchanged.

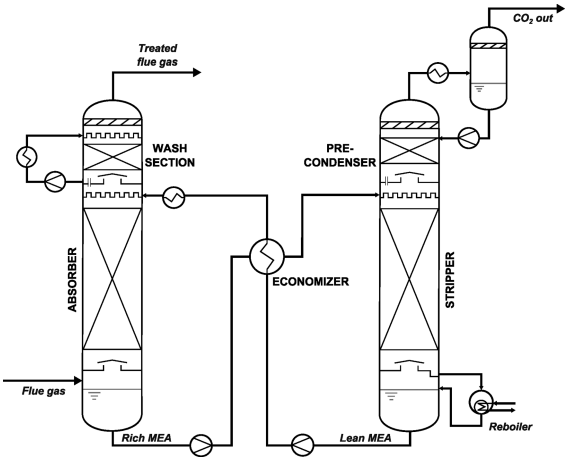

Figure 1. Process flow diagram of a typical CO_2 capture process by chemical absorption.

Process simulation is a suitable way for assessing the energy performance of several processes using different solvents before performing tests on pilot plants and building processes at an industrial scale. As absorption and stripping columns are the two main unit operations, rigorous models for these two units are needed. Several rate-based models have already been used

Received: October 11, 2012
Revised: December 14, 2012
Accepted: February 21, 2013

   dx.doi.org/10.1021/ie302768s | Ind. Eng. Chem. Res. XXXX, XXX, XXX−XXX

in the literature to model absorption and stripping columns.[7−14] All these models estimate rigorously heat- and mass-transfer fluxes with only slight differences in formulation of the rate-based equations. The main difference lies in the thermodynamic model used for representation of vapor−liquid and chemical equilibria. Dugas et al.[15] have used the Aspen Plus software to represent the behavior of the CASTOR pilot plant unit using the e-NRTL thermodynamic model. Gaspar and Cormos[13] have used the Wilson−NRF model, and Tobiesen et al.[10,16] have used an in-house model with a simplified thermodynamic model.

Such units are rate-controlled and mathematical models must properly represent both thermodynamics (chemical and phase equilibria) and chemically enhanced heat and mass transfer. A rigorous thermodynamic framework is of prime importance to allow the correct modeling of solvent in a wide range of concentration, temperature, and for different solvents. Equilibrium stage models are useful to model separation units from a global heat and mass balance point of view but are not predictive, since the height equivalent to a theoretical plate must be fitted on experiment data; however, they fail in the prediction of advanced configurations (e.g., intercooler, split-flow), where interactions between thermodynamics and rate-controlled steps are strong. Therefore, the use of a rate-based model seems mandatory to take into consideration all phenomena.

The purpose of this paper is to present a rate-based model developed for absorption and stripping columns, that is, the first step toward the modeling and parametric optimization of a complete process. Since the goal is to optimize advanced flow schemes with different solvents, the model is developed in-house, so that no additional software layer will be needed for optimization, which is not straightforward with a commercial process simulator. Communication between different software layers is not robust enough and too time-consuming for proper use in optimization. The developed model is similar to others presented in the literature, but a rigorous thermodynamic model based on local composition is used: the extended UNIQUAC framework. A sensitivity analysis is performed on the absorber and stripper in order to emphasize the most limiting phenomena (among hydrodynamics, mass-transfer, thermodynamics phenomena) for each unit. Two film models then are described, as well as complete column models for the absorber and the stripper. Insights are also given on the contribution of CO_2 and H_2O on heat fluxes between phases for the absorber and the stripper.

2. THERMODYNAMIC FRAMEWORK

CO_2 capture by chemical absorption/desorption processes relies on the preferential separation of CO_2 from flue gas in a chemical solvent. In these systems, thermodynamics is the most important factor concerning directly the potential of absorption, since it determines equilibria at the vapor/liquid interface, speciation in liquid phase, and heat of absorption. Thus, a good representation of those thermodynamic phenomena by an appropriate model is of prime importance for the correct modeling of CO_2 capture processes.

In aqueous alkanolamine solutions, in addition to molecular species such as solvents and dissolved gases, electrolyte species are present in the liquid phase. The thermodynamic model must take into consideration both phases and chemical equilibria for a wide range of amine concentration, CO_2 loading, temperature, and pressure. Several thermodynamic models have been used in the literature to represent the absorption of acid gases in alkanolamine solution, and they can be classified as one of three types: nonrigorous empirical, rigorous model based on an homogeneous approach (equation of state), or rigorous model based on an heterogeneous approach (excess Gibbs energy). The first models are called nonrigorous because they are based on empirical mathematical relations, rather than theoretical considerations. Vapor-liquid equilibria (VLE) and chemical equilibria are represented in these models by fitting numerical parameters on experimental data. The resulting correlations, such as that of Kent and Eisenberg[17] for the CO_2 partial pressure, are often easy to implement. However, there is a lack of extrapolation outside the conditions used for regression (i.e., temperature, pressure, and composition). Among more-rigorous models, one can use an homogeneous approach using an equation of state to represent both the liquid phase and the gas phase (including electrolytes) or an heterogeneous approach using the excess Gibbs energy to obtain activity coefficients in the liquid phase. Homogeneous approaches are based on the Helmholtz energy; most of the models use the formulation of Furst and Renon,[18,19] who represented acid gases absorption in a diethanolamine (DEA) solvent. Alternately, Button and Gubbins[20] used a statistical approach by extending the Statistical Associating Fluid Theory (SAFT) theory to alkanolamine systems. The third class of models uses the excess Gibbs energy to compute activity coefficients; they are often based on already-existing models for nonelectrolyte systems and extended with the Debye−Hückel theory to address electrolyte species. The model by Deshmukh and Mather[21] is one of the simpler models, and parameters have been regressed for some amines;[22] it assumes ideality for water and calculates the activity coefficient for diluted species with a virial term for interaction between species. The model by Pitzer[23] is quite similar and has been used to represent the solubility of CO_2 in aqueous methyldiethanolamine (MDEA) and piperazine (PZ).[24] Among the more elaborated models using the local composition of the mixture, the electrolyte-NRTL (e-NRTL) and extended UNIQUAC (e-UNIQUAC) models prevail. The e-NRTL model[25,26] has been extensively used for CO_2 absorption characterization.[27−29] The extended UNIQUAC[30,31] provides the same theoretical basis as e-NRTL, with a simpler formulation, and it has already proved its ability to represent the alkanolamine system for CO_2 absorption.[32,33]

In order to represent the thermodynamic behavior rigorously, the framework used in this work for the modeling of CO_2 absorption in alkanolamine solutions is based on extended UNIQUAC formulation.

2.1. Extended UNIQUAC Model. The original UNIQUAC model developed by Abrams and Prausnitz[34] relies on the geometric hypothesis of Guggenheim[35] to account for short-range interactions between molecules through a combinatorial entropic term and a residual enthalpy term in the excess Gibbs expression. Sander[30] extended this model to electrolyte systems by adding a Debye−Hückel term to account for long-range electrostatic interaction. The extended UNIQUAC framework presented by Thomsen and Rasmussen[31] has been implemented in this work.

For the monoethanolamine (MEA) system, the interaction parameters have been taken from the work of Aronu et al.,[33] whose experiments cover the widest range of concentration and temperature so far. Their parameters lead to a good representation of both speciation (chemical equilibria) and

dx.doi.org/10.1021/ie302768s | Ind. Eng. Chem. Res. XXXX, XXX, XXX−XXX

phase equilibria with average absolute relative deviations (AARDs) of 24.3% for the CO_2 partial pressure and 11.7% for the total pressure.

2.2. Chemical Equilibria. In an aqueous alkanolamine system with CO_2, the following chemical reactions occur and determine the ionic speciation of each molecular species:

Water Ionization:

$$2H_2O \rightleftharpoons HO^- + H_3O^+ \tag{1}$$

Dissociation of Carbon Dioxide:

$$CO_2 + 2H_2O \rightleftharpoons HCO_3^- + H_3O^+ \tag{2}$$

Dissociation of Bicarbonate:

$$HCO_3^- \rightleftharpoons CO_3^{2-} + H_3O^+ \tag{3}$$

Dissociation of Protonated Amine:

$$R_1R_2R_3NH^+ + H_2O \rightleftharpoons R_1R_2R_3N + H_3O^+ \tag{4}$$

Carbamate Reversion (Primary and Secondary Amines):

$$R_1R_2R_3NCOO^- + H_2O \rightleftharpoons R_1R_2R_3N + HCO_3^- \tag{5}$$

Those equilibria can be solved using two numerical methods: the stoichiometric method and the nonstoichiometric method. The stoichiometric method consists of simultaneously solving the equations defined by the mass balances and equilibrium constants by a nonlinear solver (e.g., with a Newton-based method), which requires a good initialization. The nonstoichiometric method implemented in this work is a more straightforward way of solving chemical equilibria; the problem is formulated as a minimization of the total molar Gibbs energy submitted to mass balances, for a fixed temperature and pressure.

The chemical equilibria problem is solved by finding the molar composition, minimizing the total Gibbs energy submitted to mass balances (expressed here as element balances to reduce the number of constraints):

$$\min_{\mathbf{n}} G = \min \sum_{i=1}^{N_C} n_i \mu_i \tag{6}$$

subject to

$$\mathbf{A}\cdot\mathbf{n} = \mathbf{b} \tag{7}$$

with the following chemical potentials:

$$\mu_i(\mathbf{n}, T) = \mu_i^0(T) + RT \ln \frac{\gamma_i n_i}{n_t} \tag{8}$$

where $\mathbf{A}$ is the $(N_E \times N_C)$ element matrix, i.e., A_{ki} is the number of k atoms in compound i; $\mathbf{n}$ is the N_C composition vector; $\mathbf{b}$ is the N_E vector of total amount of each element in the mixture; μ_i^0 is the standard-state chemical potential of compound i; and n_t is the total mole number ($n_t = \sum_{i=1}^{N_C} n_i$). The electroneutrality relation could be added as another constraint, but it is not mandatory if this equation is dependent on mass balance.[29]

Before minimizing the Gibbs energy, the standard-state chemical potentials must be evaluated at a fixed temperature. Some reference potentials are available in the literature, but not for the alkanolamine system. However, correlations for equilibrium constants are available for reactions 1−5 and give good information on the temperature dependence of standard-state potentials. Indeed, the N_R equilibrium constants can be expressed with respect to the standard-state chemical potentials:

$$RT \ln K_k(T) = -\sum_{i=1}^{N_C} \nu_{ik} \mu_i^0(T) \qquad k = 1, ..., N_R \tag{9}$$

Thus, knowing N_R relations between the standard-state chemical potentials, a total of $(N_C - N_R)$ variables must be fixed to obtain a fully determined system. The simplest way is to take them equal to zero. The standard-state chemical potentials can be expressed as follows:

$$\mu^0(T) = -RT \begin{bmatrix} \nu^T \\ \mathbf{E} \end{bmatrix}^{-1} \begin{pmatrix} \ln \mathbf{K}(T) \\ \mathbf{0} \end{pmatrix} \tag{10}$$

where ν is the stoichiometry matrix and $\mathbf{E}$ is a $(N_C - N_R) \times N_C$ matrix filled with zeros, except for one element that is equal to 1 per line, to identify the base component to be taken as null. This way, all standard chemical potentials are determined and consistent with the definition of each equilibrium constant (see eq 9).

Knowing the reference chemical potentials, the total Gibbs energy can be minimized to obtain the composition at chemical equilibrium. The linearly constrained minimization problem defined by eq 7 can be reduced to an unconstrained minimization problem by incorporating the equality constraints defined by element balances into the objective function considered as the Lagrangian. It is required that the Lagrangian gradient, with respect to Lagrange multipliers and composition, be equal to zero at the minimum.

Smith and Missen[36] proposed an efficient algorithm to minimize the Lagrangian function for an ideal solution, Austgen[37] applied it for nonideal systems with an outer loop on activity coefficients. The algorithm implemented in this work is based on the Greiner[38] method, as detailed by Michelsen and Mollerup,[39] which extends the Smith and Missen algorithm to nonideal behavior. The iterative algorithm adopted here exploits the fact that constraints are linear to obtain the values of Lagrange multipliers for the current composition estimation; new estimates are then computed and the procedure is repeated until convergence, with respect to the mole number.

2.3. Phase Equilibria. At a given temperature and pressure, VLE are described through equality of liquid and vapor chemical potentials for each compound, which can be formulated as follows:

$$\mu_i^{liq}(T, P, \mathbf{n}) = \mu_i^{vap}(T, P, \mathbf{n}) \tag{11}$$

Because of the choice of an excess Gibbs model to represent the nonideal behavior of the liquid phase, liquid chemical potentials are expressed with activity coefficients as detailed above. In the heterogeneous approach, the vapor phase is represented through an equation of state; the Peng−Robinson equation of state is used in this work to calculate the gas-phase properties, especially the fugacity coefficients. Within this framework, eq 11 becomes

$$y_i = K_i^{VLE} x_i \tag{12}$$

where the equilibrium constant for volatile species (e.g., water and amines) is given as

dx.doi.org/10.1021/ie302768s | Ind. Eng. Chem. Res. XXXX, XXX, XXX−XXX

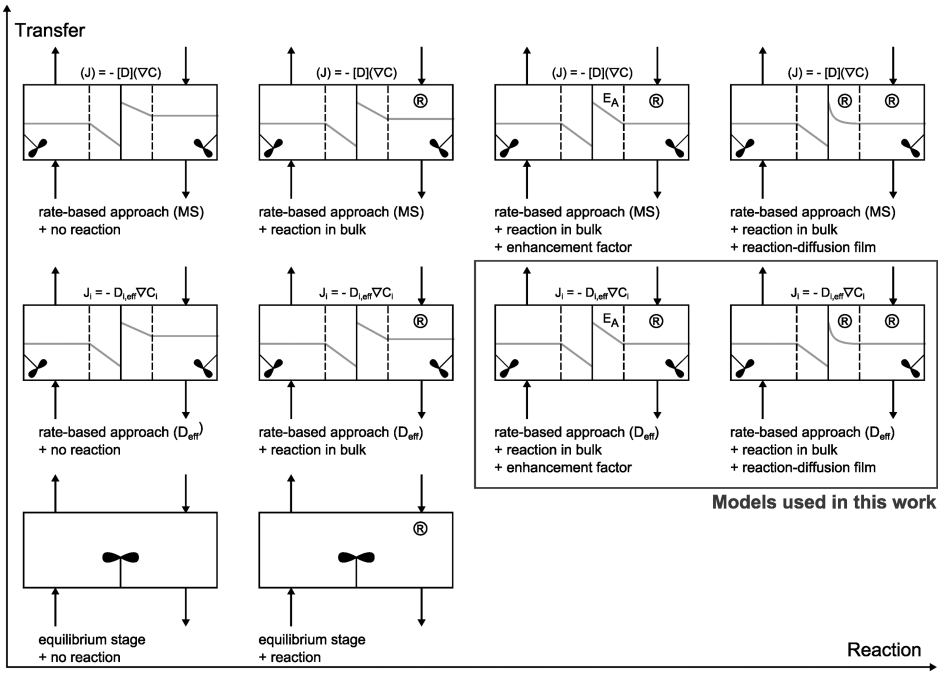

Figure 2. Overview of modeling approaches for reactive separation units.

$$K_i^{\mathrm{VLE}} = \frac{\gamma_i x_i \varphi_i^{\mathrm{sat}} P_i^{\mathrm{sat}}}{\varphi_i P} \exp\left[\frac{v_i(P - P_i^{\mathrm{sat}})}{RT}\right] \tag{13}$$

For solutes (CO_2, O_2, N_2), Henry's law at infinite dilution is used:

$$K_i^{\mathrm{VLE}} = \frac{\gamma_i x_i \mathcal{H}_i^{\infty}}{\varphi_i P \gamma_i^{\infty}} \exp\left[\frac{v_i^{\infty}(P - P_{\mathrm{H_2O}}^{\mathrm{sat}})}{RT}\right] \tag{14}$$

with φ_i being the fugacity coefficient of compound i in the gas phase, φ_i^{sat} is the saturated vapor fugacity coefficient, P_i^{sat} is the vapor pressure, and v_i and v_i^{∞} are, respectively, the partial molar volume and infinite dilution partial molar volume. The exponential term is the Poynting factor, which is used for pressure correction; $\mathcal{H}_i^{\infty}$ is Henry's coefficient at infinite dilution and γ_i^{∞} is the infinite dilution activity coefficient (calculated by e-UNIQUAC model). Note that the e-UNIQUAC model gives asymmetrical activity coefficients; therefore, the activity coefficient of amine must be converted for proper use in eq 13.

3. MASS-TRANSFER MODELS

Absorption and stripping are complex unit operations where numerous phenomena such as diffusion, reaction, and interfacial mass and energy transfer take place and interact with each other. Moreover, they are coupled with nonideal thermodynamic behavior. These units are rate-controlled, and mathematical models must solve mass and energy balances for each phase to properly evaluate the mass and energy transfer fluxes through the gas/liquid interface. A rate-based model inherently requires more computation power and information on physical properties than an equilibrium model, but it ensures a better representation and allows proper design of equipment.

3.1. Selection of Model Complexity. Several rate-based models have been used in the literature to model CO_2 capture processes; most of them focus on absorption columns,[7−11,14] and a few deal with stripping.[12,13,16] Among these models, different approaches are possible, according to the degree of complexity used for each submodel (i.e., for each phenomenon to tackle). In addition to the thermodynamics already detailed in the previous section, one must consider mass transfer as well as reactions and hydrodynamics. Noeres et al.[40] and Kenig et al.[41] have given good reviews of the different approaches for reactive absorption and reactive distillation, which also applies to reactive stripping. Noeres et al.[40] distinguished the modeling approaches for reactive absorption and reactive distillation according to the degree of complexity chosen for the representation of hydrodynamics, reaction kinetics, and mass transfer. Figure 2 gives an overview of the modeling approaches available for reaction and mass transfer in reactive separation.

The role of the interfacial transfer model is to provide the values of mass and energy fluxes (N_i/q), knowing the bulk temperatures and concentrations provided by the transport model. The gas−liquid mass transfer involves two phenomena: the molecular diffusion caused by random movement of molecules (Brownian and turbulent flow) and the convective transport due to the overall movement of matter. Mass transfer fluxes are then obtained by summing the diffusive and convective terms:

$$N_i = J_i + x_i \sum_{i=1}^{N_C} N_i \tag{15}$$

Heat Transfer. Energy fluxes are calculated using the Chilton−Colburn analogy to calculate the heat-transfer coefficient (h) from the mass-transfer coefficient. Since the liquid and gas temperatures are quite close, because of turbulence in bulks, thermal profiles are assumed to be linear in each film, so that interfacial models concentrate on the determination of mass-transfer fluxes.

$$q^{\mathrm{G}} = h(T^{\mathrm{G}} - T^{\mathrm{L}}) \tag{16}$$

dx.doi.org/10.1021/ie302768s | Ind. Eng. Chem. Res. XXXX, XXX, XXX−XXX

$$q^{L} = h(T^{G} - T^{L}) + \sum_{i=1}^{N_C} N_i^{L} \overline{H}_i^{L} \tag{17}$$

Hydrodynamics. In separation columns, hydrodynamics is often simplified by a plug-flow assumption for both the gas and liquid phases. But hydrodynamics does not follow an ideal flow behavior, since axial and radial dispersion occur in an industrial column. To take this aspect into consideration, Higler et al.[42] proposed a multiple cell approach to model nonideal behavior in trays for reactive separation processes. Hydrodynamics can also been characterized by means of CFD modeling, which has proven to be useful for the study of packed column performances.[43] However, because of the large calculation times needed for 3D simulations, CFD modeling should be reserved for the characterization of hydrodynamics, rather than for operating modeling purposes. Furthermore, since all correlations for mass-transfer coefficients are given under the plug-flow assumption, this simplification remains intensively used in reactive separation unit models.

Diffusion. Diffusion mechanisms in multicomponent systems involve the driving force as a concentration gradient. In some cases, interaction effects between driving forces can lead to counterintuitive behavior such as reverse diffusion, osmotic diffusion, or diffusion barriers.[44]

The Maxwell−Stefan equations offer a fundamentally sound way to represent multicomponent mass diffusion by linking diffusion fluxes to a generalized driving force. This driving force accounts for all the forces tending to move each species in the solution, and especially the effect of a chemical potential gradient. In electrolytic systems, an electrostatic term can be added to the driving force, but this term has no influence on the mass transfer in alkanolamines systems (see the work of Benjelloun-Dabagh et al.[45]).

Alternatively, the effective diffusivity method can be used. In this approach, interactions between concentration gradients are neglected and diffusion equations are written as a generalized Fick's law. In dilute electrolyte systems, the effective diffusivity method has proven to be a suitable simplification of the Maxwell−Stefan general equations,[44,46] hence its use in this work. The Maxwell−Stefan formulation would be more adapted in other applications such as membrane processes.[47]

Reaction Kinetics. In reactive absorption and stripping, rate-controlled reactions occur in liquid films; this leads to a chemical enhancement of the mass transfer by increasing the driving force. In the liquid film, diffusion and reaction mechanisms are coupled and must be taken into consideration together. Both aspects can be represented by using an enhancement factor to estimate the influence of chemical reactions on mass transfer, or, alternatively, by solving the mass balance in the direction of transfer with the full reaction scheme. These two approaches are investigated in this work, and their numerical formulation and solution are described in the next sections.

In this work, the effective diffusivity method is used to model mass transfer; hydrodynamics is modeled using correlations. Reaction kinetics are modeled with both an enhancement factor and reaction-diffusion approaches and compared in the discussion part.

3.2. Diffusion-Reaction Film Model. The first approach consists of solving the mass balance in the direction of transfer by taking into consideration the diffusion equations coupled with the full reaction scheme. The mass balance along the diffusion path gives for each compound:

$$\frac{\partial c_i}{\partial t} + \frac{\partial N_i}{\partial \xi} = \mathcal{R}_i \qquad i = 1, ..., N_C \tag{18}$$

where ξ is the spatial coordinate in film varying from 0 to the film thickness δ, and $\mathcal{R}_i$ is the production rate of i by chemical reactions.

$$\mathcal{R}_i = \sum_{k=1}^{N_R} \nu_{ik} r_k \qquad i = 1, ..., N_C \tag{19}$$

These partial differential equations are simplified by neglecting the convective flux for the expression of N_i and assuming steady state, hence the system of ordinary differential equations (ODEs)

$$0 = D_{i,\mathrm{eff}}^{L} \frac{\partial c_i}{\partial \xi} + \mathcal{R}_i \qquad i = 1, ..., N_C \tag{20}$$

submitted to the boundary conditions at the gas/liquid interface (continuity of fluxes):

At $\xi = 0$:

$$-D_{i,\mathrm{eff}}^{L} \frac{\partial c_i}{\partial \xi}\bigg|_{\xi=0} = k_{i,\mathrm{eff}}^{G} c_t^{G} \left(y_i^{B} - K_i^{\mathrm{VLE}} \frac{c_i}{c_{\mathrm{tot}}^{L}}\bigg|_{\xi=0} \right)$$
$$i = 1, ..., N_C \tag{21}$$

For nonvolatile species (i.e., ions), the second term is null.

At the interface between the liquid film and the bulk, the boundary conditions are

At $\xi = \delta$:

$$c_i = c_i^{B} \qquad i = 1, ..., N_C \tag{22}$$

This model has extensively been used to represent the absorption of acid gases,[10,45] but also for determining the kinetic parameters for gas−liquid reactive absorption.[48,49] The knowledge of the film thickness (δ) is needed to integrate along the diffusion film. This thickness depends on the species but can be estimated by considering the diffusion of $MEACOO^-$ and assuming that the film thickness is not modified by chemical reactions:[50]

$$\delta = \frac{k_{\mathrm{MEACOO^-,eff}}^{L}}{D_{\mathrm{MEACOO^-,eff}}^{L}} \tag{23}$$

Equations 20−22 define a two-point boundary value problem. The orthogonal collocation method[51] is used to transform the set of ODEs (eq 20) into a set of algebraic equations. The resulting system of nonlinear equations is solved using the FORTRAN routine HYBRD from the MINPACK library,[52] which is based on a modification on a hybrid Powell method.

3.3. Enhancement Factor Model. Rather than solving coupled diffusion-reaction equations along the film thickness, some analytical solutions can be used by means of an enhancement factor. The latter modifies the liquid mass-transfer coefficients to take into account the enhancement of the gas−liquid transfer due to chemical reaction, i.e., coefficients are expressed by

$$k_{i,\mathrm{eff}}^{L,*} = E_i k_{i,\mathrm{eff}}^{L} \qquad i = 1, ..., N_C \tag{24}$$

dx.doi.org/10.1021/ie302768s | Ind. Eng. Chem. Res. XXXX, XXX, XXX−XXX

where $k^{L}_{i,eff}$ is the mass-transfer coefficient on the liquid side without reaction (hydrodynamic correlations), E_i the enhancement factor for compound i, and $k^{L,*}_{i,eff}$ the mass-transfer coefficient with chemical enhancement; for nonreactive compounds, the enhancement factors must be assumed to be equal to unity. The problem is thus reduced to the calculation of the enhancement factor whose expression depends on the chemical reactions involved (i.e., multiple or single, reversible or irreversible reactions).

For a second-order reversible reaction (first-order with respect to CO_2), the formulation from ref 53 can be used:

$$E_{CO_2} = \frac{-Ha^2}{2(E^\infty - 1)} + \sqrt{\frac{-Ha^4}{4(E^\infty - 1)^2} + \frac{E^\infty Ha^2}{E^\infty - 1} + 1} \tag{25}$$

where Ha is the Hatta number, which describes the chemical regime for a pseudo-first-order reaction of overall kinetics $r_{ov} = k_{ov}[CO_2][Am]$,

$$Ha = \frac{\sqrt{D_{CO_2,eff} k_{ov}[Am]}}{k^{L}_{CO_2,eff}} \tag{26}$$

and E^∞ is the enhancement factor for the corresponding instantaneous equilibrium reaction. An overview of several expressions for single and multiple instantaneous reversible reactions has been given by Chang and Rochelle.[54] For a reversible single reaction (A + B ⇌ C + D), the infinity instantaneous enhancement factor of Olander[55] is used in this work:

$$E^\infty = 1 + \frac{D_{C,eff}}{D_{A,eff}}\left(\frac{x^{I}_{C} - x^{B}_{C}}{x^{I}_{A} - x^{B}_{A}}\right) \tag{27}$$

Note that interfacial concentrations are needed for the calculation of the instantaneous enhancement factor. It results in an iterative procedure based on the solution of the algebraic system defined by continuity of fluxes between the gas phase and the liquid phase (eqs 28 and 29), coupled with summation equations (eqs 30 and 31) and an equation describing the VLE (eq 32).

$$0 = N_i - N^{L}_i \qquad i = 1, ..., N_C - 1 \tag{28}$$

$$0 = N_i - N^{G}_i \qquad i = 1, ..., N_C - 1 \tag{29}$$

$$0 = 1 - \sum_{i=1}^{N_G} y^{I}_i \tag{30}$$

$$0 = 1 - \sum_{i=1}^{N_C} x^{I}_i \tag{31}$$

$$0 = y^{I}_i - K^{VLE}_i x^{I}_i \qquad i = 1, ..., N_G \tag{32}$$

where the mass-transfer fluxes on each side are

$$N^{L}_i = -c^{L}_{tot} E_i k^{L}_{i,eff}(x^{I}_i - x^{B}_i) + x^{B}_i \sum_{j=1}^{N_C} N^{L}_j \qquad i = 1, ..., N_C \tag{33}$$

$$N^{G}_i = -c^{G}_{tot} k^{G}_{i,eff}(y^{B}_i - y^{I}_i) + y^{B}_i \sum_{j=1}^{N_G} N^{G}_j \qquad i = 1, ..., N_C \tag{34}$$

Knowing the bulk concentrations, the $2N_C + N_G$ unknowns are the mass-transfer fluxes N_i and interfacial mole fractions on liquid and gas side x^{I}_i and y^{I}_i. This nonlinear algebraic system is also solved by the FORTRAN routine HYBRD from the MINPACK library.[52]

4. RATE-BASED COLUMN MODEL

The previous part describes the solution of two different film models that can calculate the transferred heat and mass fluxes by knowing the concentrations and the temperature in liquid and gas bulks. The rate-based column model relies on the integration of energy and mass transfer fluxes exchanged along the absorber path, which is performed through one of the two stand-alone film models presented earlier and called for each position along the packing height.

4.1. Transport Equations. The transport model assumes an adiabatic column where the liquid and gas follow a plug-flow hydrodynamic regime without axial dispersion. Reactions are assumed to be at equilibrium only in the bulk and are rate-controlled in the film. Transport equations are solved only on apparent species (i.e., molecular species with associated ions); to reduce the amount of equations, steady-state conditions are considered in this work. Figure 3 shows a schematic

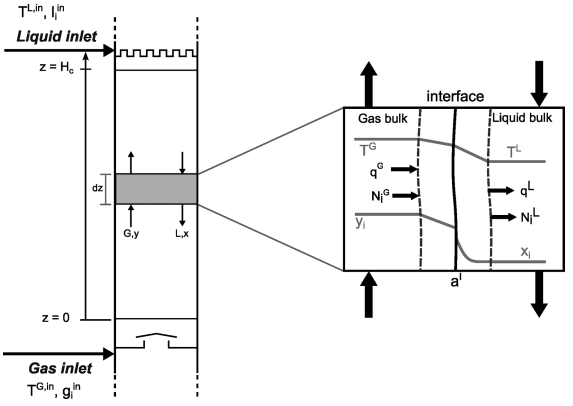

Figure 3. Two-film model on a differential packing element.

representation of the integration of a differential packing element along the column height. The two-film theory used for the modeling of rate-based columns assumes that each phase is composed of a perfectly mixed bulk and a laminar film adjacent to the interface.

The $2(N_{gaz} + 1)$ transport equations are composed of heat and mass balances for each bulk:

$$0 = \frac{dL_i}{dz} + N^{L}_i a^{I} A_c \qquad i = 1, ..., N_C \tag{35}$$

$$0 = \frac{dG_i}{dz} + N^{G}_i a^{I} A_c \qquad i = 1, ..., N_C \tag{36}$$

$$0 = L_{tot} C^{L}_p \frac{dT^{L}}{dz} + q^{L} a^{I} A_c \tag{37}$$

dx.doi.org/10.1021/ie302768s | Ind. Eng. Chem. Res. XXXX, XXX, XXX–XXX

$$0 = G_{tot} C_p^G \frac{dT^G}{dz} + q^G a^I A_c \quad (38)$$

with the boundary conditions at the inlet and outlet of packing:

$z = 0$:

$$T^G = T^{G,in} \quad \text{and} \quad G_i = G_i^{in} \qquad i = 1, ..., N_C \quad (39)$$

$z = H_c$:

$$T^L = T^{L,in} \quad \text{and} \quad L_i = L_i^{in} \qquad i = 1, ..., N_C \quad (40)$$

4.2. Absorber Model. Since an absorber is composed of a packing where the flue gas and the solvent exchange mass and energy are in a counter-current flow, the absorber model simply consists of solving the transport model described above. The numerical problem is thus described by the set of ODEs described by eqs 35−38, subject to the boundary conditions described in eqs 39 and 40.

In the same way as for the diffusion-reaction problem, this set of ODEs is transformed to a set of algebraic equations by means of the orthogonal collocation method;[51] the resulting system is solved by the FORTRAN routine HYBRJ from the MINPACK library.[52] Since the Jacobian matrix is sparse, computational effort is saved by supplying only the nonzero elements of the matrix, calculated by finite differences.

4.3. Stripper Model. The stripper model is similar to the absorber model with an increased complexity due to recycle loops from the reboiler and the condenser. The gas exiting the packing is condensed and the condensate is returned back to the top of the packing. The bottom liquid outlet is partially vaporized in the reboiler and the resulting gaseous phase defines the bottom gas inlet of packing. Moreover, the heat duty provided in reboiler must be adapted to regenerate the same flow rate of CO_2 as the amount absorbed in the absorber (defined by lean loading at the bottom of stripper). The stripping section is described by the same equations as the absorber model, i.e., the transport equations on the packing, as well as the precondenser (packing above stripping section). The condenser is modeled as a TP-flash and the reboiler is modeled as a QP-flash.

For the stripper calculation, the diffusion-reaction film model is not used, since it requires a finite rate of reaction and no kinetic law is available under these operating conditions. Considering the high temperature of stripping column, reactions are supposed at equilibrium and only the infinity instantaneous enhancement factor is used (see eq 27).

Two approaches can be adopted for the solution of the stripper model: a sequential procedure or an equation-oriented approach. The sequential approach uses successive calls to different submodels until convergence of output fluxes, whereas the equation-oriented approach consists of solving all the equations describing this unit operation simultaneously.

The convergence scheme of the sequential method is summarized as follows:

(1) Choose an initial heat duty Q_{reb} and estimate the gas inlet (output of reboiler);
(2) Solve transport equations for packing (see the absorber model);
(3) Solve precondenser and condenser (TP-flash) to get the new liquid input;
(4) Solve reboiler (QP-flash) to get the new gas input;
(5) Check convergence regarding the total molar flux leaving the stripper; if not, return to step 2;
(6) Check convergence on lean loading; if not, adapt heat duty Q_{reb} and return to step 2; and
(7) Compute output fluxes.

Note that numerical second-order filters have been added at both inlets of stripping packing (steps 3 and 4), to smooth the changes in composition and temperature; more iterations are consequently needed, but it does allow a more stable convergence of the column. The adaptation of the heat duty necessary to control the amount of regenerated CO_2 provided in the reboiler is performed with a simple secant method, bounded by heat duty at bubble and dew points, to ensure that (i) steam is produced in the reboiler and (ii) all the solvent is not totally vaporized.

The equation-oriented approach requires a proper initialization of all variables. As the reboiler heat duty is adjusted to fulfill a desorption objective, the main output variables are known and the initialization procedure exploits this fact to generate initial profiles.

Both approaches were investigated in this work and it appears that the equation-oriented approach is faster and more robust than the sequential procedure; therefore, this approach has been kept in this work.

5. COMPARISON WITH EXPERIMENTAL RESULTS

Several sets of data are available in the literature for CO_2 absorption/stripping units.[56] Experimental results from the Esbjerg pilot plant (FP-7 European project CASTOR) and additional data from Tobiesen et al.[10] for the absorber have been chosen to validate the model. The Esbjerg CASTOR pilot plant was a conventional absorption/stripping process, similar to the one pictured in Figure 1, and the results presented here were obtained during the second MEA campaign.

Simulation results presented in this section were performed with the enhancement factor film model. The comparison with the diffusion-reaction film model is performed in the Discussion section. Correlations used for the calculation of physical properties are reported in Table 1.

The first test performed during the CASTOR campaign intended to optimize the solvent flow rate at 90% CO_2 removal (Run 1A to Run 1E); the stripper pressure was fixed at 1.85 bar(a) and the reboiler temperature (i.e., the reboiler heat duty)

Table 1. List of References for the Calculation of Physical Properties

property	reference
liquid viscosity	57
vapor viscosity	58
liquid density	57
vapor density	59
surface tension	60
gas diffusion coefficients	61
liquid diffusion coefficients	62
ionic diffusion coefficients	63
Henry's constant	27
heat of vaporization	64
aqueous heat capacity	64
ideal gas heat capacity	65
reaction rate	48
equilibrium constants	27
wet interfacial area	66
mass-transfer coefficients	66

dx.doi.org/10.1021/ie302768s | Ind. Eng. Chem. Res. XXXX, XXX, XXX−XXX

was adjusted to achieve a given removal efficiency of 90%. The objective of the second test (Run 2A to Run 2C) was to determine the steam consumption needed to achieve given removal efficiency for a fixed stripper pressure of 1.85 bar(a). In the third test (Run 3A to Run 3D), the influence of the stripper pressure at 90% CO_2 removal (by adjustment of reboiler temperature) was studied with a flow rate fixed at a simulated optimal value.

The two next sections compare the simulations of each column (absorber and stripper) separately with these three tests, and the third one addresses the energy performance of the entire process to assess the model representativeness more relevantly.

5.1. Absorber Validation. The absorption section of the Esbjerg pilot plant is constituted by a 17-m-height and 1.1-m-diameter packed section filled with IMTP-50, and the column operates at atmospheric pressure. The solvent used is an aqueous solution of ~30 wt % monoethanolamine (MEA). Several solvent flow rates were applied in pilot plant tests, and the removal efficiency as well as rich and lean loadings were reported.[15]

However, experimental uncertainties complicate the model validation. Indeed, there is a difference between the experimental values obtained for the CO_2 absorbed in the gas phase, the CO_2 dissolved in the liquid phase, and the CO_2 desorbed in the gas phase with an average relative deviation of ~6% for all 12 tests for the CASTOR pilot plant.

In addition to CASTOR pilot plant measurements, data from Tobiesen et al.[10] have been used for validation, since a wider range of inlet gas CO_2 concentration is covered (dry molar fraction from 1.6% to 15.3%) and another packing was used (Mellapak 250Y).

For validation purposes, the variables that are taken to be equal to the experimental measurements are the solvent flow rate, temperature, and lean loading ratio, as well as the specifications of the flue gas entering the absorber (i.e., the liquid and gas inlet streams). The simulated CO_2 removal efficiency is compared with pilot plant measurements in Figure 4. Average absolute deviations of 0.007 mol CO_2/mol MEA and 1.3% are respectively obtained for the rich loading ratio and the CO_2 removal efficiency. The trends numerically obtained are in excellent agreement with those experimentally observed. The deviations are slightly higher for the CASTOR pilot plant than for the laboratory pilot plant; this is not surprising, since

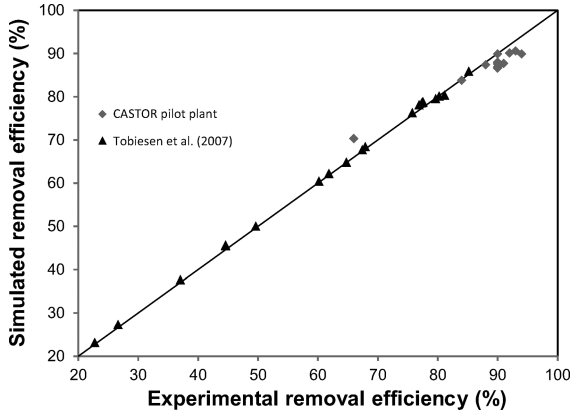

Figure 4. Comparison between the experimental and simulated CO_2 removal efficiency from the work of Tobiesen et al.[10] and the CASTOR pilot plant.

experimental conditions are better managed and more-accurate measurements are possible at a laboratory scale. Uncertainties on industrial measurements are mainly due to variations of flue gas conditions from the power plant, whereas inlet conditions are more stable at laboratory scale.

Figure 5 represents the temperature and concentration profiles along the absorber for Run 1A at the CASTOR pilot

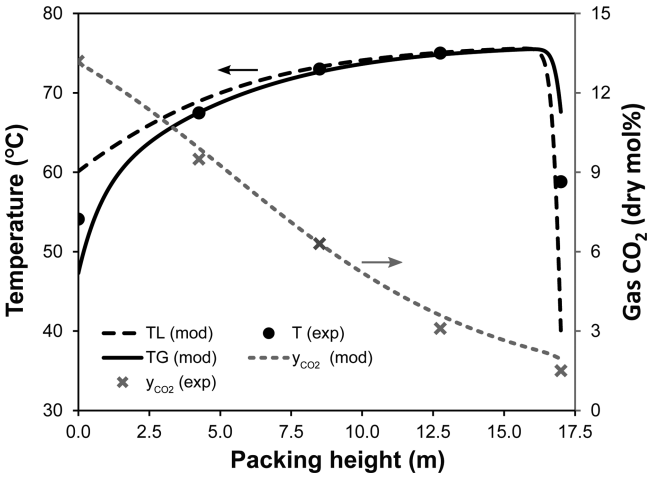

Figure 5. Comparison of absorber temperature and concentration profiles between simulations and experiments for Run 1A at the CASTOR pilot plant.

plant, corresponding to a high lean loading value. Temperature profiles at the top of the packing are quite stiff; this is mainly due to the high reaction rate, coupled with the high driving force caused by the amount of free MEA available. In addition, water condenses due to cold solvent, releasing its latent heat in the liquid phase. Both temperature and concentration profiles are very close to experimental measurements.

Figure 6 represents the temperature and concentration profiles along the absorber for Run 7 from the work of

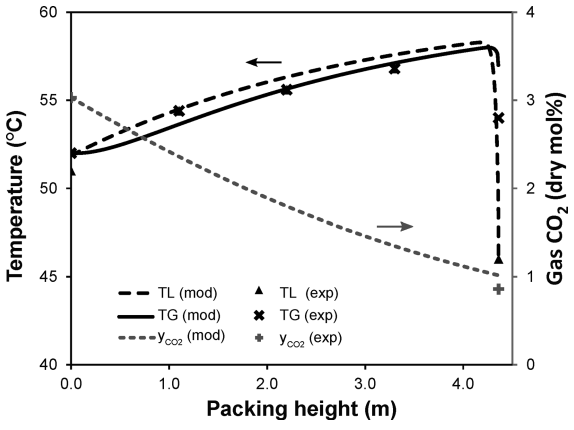

Figure 6. Comparison of the absorber temperature and concentration profiles between simulations and experiments from Run 7 in the work of Tobiesen et al.,[10]

Tobiesen et al.[10] Here again, the simulated temperature and CO_2 concentration are very close to experiments measurements.

Despite some experimental discrepancies (e.g., the mass balances are not completely verified using the experimental

dx.doi.org/10.1021/ie302768s | Ind. Eng. Chem. Res. XXXX, XXX, XXX–XXX

Table 2. Stripper Operating Conditions in the CASTOR Pilot Plant and Comparison of Reboiler Heat Duty

	parameter	Run 1A	Run 1B	Run 1C	Run 1D	Run 1E	Run 2A	Run 2B	Run 2C	Run 3A	Run 3B	Run 3C	Run 3D
pilot plant	P_{reb} (bar(a))	1.85	1.85	1.85	1.85	1.85	1.85	1.85	1.85	2.19	1.85	1.50	1.23
	α_{lean}	0.27	0.25	0.22	0.19	0.17	0.19	0.22	0.27	0.21	0.21	0.22	0.24
	α_{rich}	0.45	0.46	0.47	0.47	0.47	0.46	0.46	0.47	0.46	0.47	0.46	0.45
	Q_{reb} (GJ/t CO_2)	3.90	3.72	3.73	3.63	3.75	3.84	3.83	3.91	3.74	3.69	4.01	4.19
model	Q_{reb} (GJ/t CO_2)	4.11	3.86	3.93	4.46	5.33	4.61	3.99	3.86	3.86	4.99	4.55	5.30
relative deviation (%)		5	4	5	23	42	20	4	−1	3	35	13	26

values of the CO_2 flow rates), the absorber model correctly represents the trends in the range of investigated parameters and provides a good representation, with respect to experimental values obtained on the absorber.

5.2. Stripper Validation. The stripping section of the Esbjerg pilot plant is constituted by a 10-m-height, 0.8-m-diameter packed section filled with IMTP-50, operating above atmospheric pressure. In this unit, the heat duty provided in the reboiler is adjusted in order to regenerate the same amount of CO_2 as that which was absorbed. A precondensing section (height of packing = 3 m) placed between the condenser recycle and the top of the stripping section (Figure 1) recovers some of the heat of condensation that is otherwise lost in the condenser.

Table 2 summarizes the main operating parameters tested in the CASTOR pilot plant. Simulations have been performed by fixing the rich loading ratio and solvent flow rate at the experimental values, and the reboiler heat duty has been adjusted to fulfill the specification on lean loading ratio.

Several sources of experimental uncertainties exist for the reboiler heat duty, which could explain the deviations obtained between simulations and experiments. The specific reboiler heat duty (expressed in units of GJ/t CO_2) is experimentally determined by the measurement of the steam flow rate feeding the reboiler corrected by the measurement liquid flow rate leaving the reboiler, the resulting heat duty is then divided by the measurement of CO_2 desorbed. Furthermore, as explained by Tobiesen et al.,[16] the state of the rich solvent (single or two-phase) cannot be measured, leading to other experimental uncertainties. It has been assumed that the inlet rich stream is at equilibrium and not necessarily purely liquid.

Simulation results are also presented in Table 2, and the comparison between experimental and simulated temperature profiles along the stripper for Run 1B of the CASTOR pilot plant is presented in Figure 7. It appears that the model systematically overpredicts the reboiler heat duty, with an average relative deviation of 15%. Luo et al.[56] compared different simulations codes with respect to the CASTOR pilot plant and showed that three of the four codes that have been tested systematically overpredict the reboiler duties. This can be partially explained by the fact that measured rich loading ratios are low, compared to values recalculated from the gas-phase mass balance (reported in the work of Dugas et al.[15]). Consequently, less CO_2 is available in rich solvent with regard to the solvent flow rate and the amount of CO_2 absorbed in the gas phase; more energy is thus required to regenerate the same given amount of carbon dioxide, because of the lower driving force.

Nevertheless, the trends observed in the evolution of reboiler heat duty, as a function of lean loading, are similar between experiments and simulations. The trend observed for the

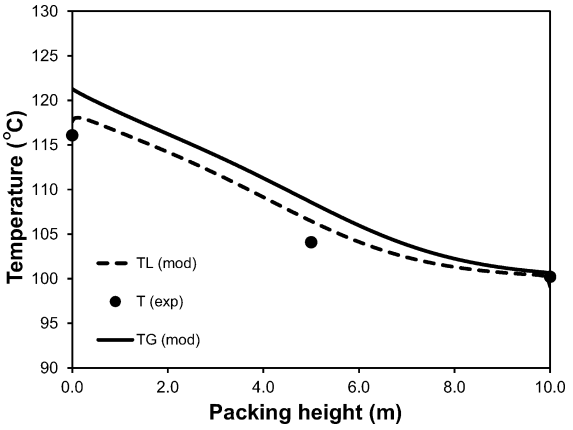

Figure 7. Comparison of stripper temperature profiles between simulations and experiments for Run 1B in the CASTOR pilot plant.

influence of the stripper pressure on reboiler heat duty is also in agreement with experimental data (Runs 3A−3D): an increase in stripper pressure leads to a reduction of reboiler heat duty. The large deviations between simulations and experiments for Runs 3A−3D can also been explained by the choice for the experimental solvent flow rate. Indeed, this solvent flow rate is chosen at an optimal value, leading to a minimum reboiler heat duty for the considered stripper pressure, which is not equal to the optimum simulated flow rates. Therefore, simulations performed are not necessarily close to the energetic minima.

In order to circumvent those discrepancies, a more relevant approach for the code validation consists of considering the entire process and in the comparison of the energetic minima for each stripper pressure, rather than comparing specific operating points. This way, the experimental uncertainties are not considered in the model and only energy performances are compared.

5.3. Evaluation of Energy Performance. In this part, the energy performance of a simple absorption/desorption loop is evaluated, based on the two unit operations validated above. The economizer between the absorber and the stripper has been simulated by a simple cross-flow heat exchanger model with a thermal pinch of 10 K (which is the value observed during the CASTOR pilot plant tests). Mellapak 250Y has been chosen as packing for both the absorber and the stripper (respectively 17 and 10 m in height). For a given solvent and a fixed removal efficiency, the heat duty at the reboiler is mainly a function of the lean loading (or solvent flow rate) and the pressure in the stripper. Consequently, simulations are performed for different lean loadings and stripper pressures; the solvent flow rates are adjusted to achieve a CO_2 removal efficiency of 90%. The heat duty is adjusted to desorb the same amount of CO_2 as that absorbed in the absorber. Results are

dx.doi.org/10.1021/ie302768s | Ind. Eng. Chem. Res. XXXX, XXX, XXX−XXX

presented in Figure 8. As noted earlier, the reboiler heat duty reaches a minimum as the lean loading increases; the curve

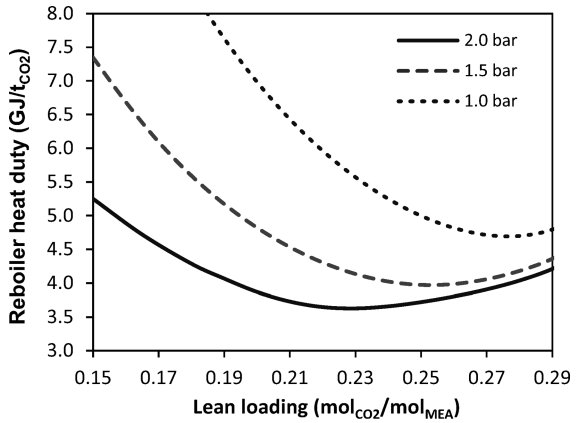

Figure 8. Simulated reboiler heat duty as a function of lean loading for different stripper pressures.

keeps a similar shape for the different pressures but moves toward low lean loadings and low heat duties.

In order to explain this evolution, it is common to describe the reboiler heat duty as a sum of three terms: Q_{sens}, which is the sensible heat needed to heat the solvent from the stripper top temperature to the reboiler temperature; Q_{strip}, which is the heat necessary to produce the stripping steam, which does not condense along the packing; and Q_{des}, which is the heat required to desorb CO_2 (including chemical reaction, physical solubility, and nonideal mixing). The sensible heat term has been calculated by integration of the liquid heat capacity from the top of the packing to the bottom (reboiler). The desorption term can be estimated with the VLE model and the Gibbs–Helmholtz relation; however, this method does not give accurate approximations.[67] This term is thus calculated with the method proposed by Le Bouhelec et al.,[68] which is based on a rigorous internal energy balance. The stripping term is calculated by subtraction of the two last terms from the total reboiler heat duty. Each term has been evaluated as a function of lean loading ratio for the highest and lowest pressures and the distribution between them is presented in Figure 9.

Based on this decomposition, it appears that the desorption term is practically constant in the range of loadings considered. Therefore, the minimum reboiler heat duty observed at a

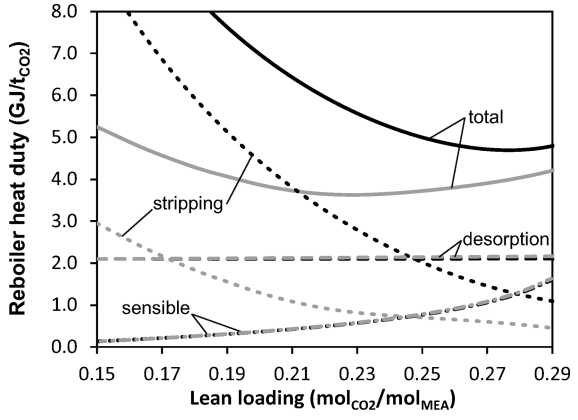

Figure 9. Decomposition of the reboiler heat duty as a function of lean loading at 1.0 bar (black line) and 2.0 bar (gray line).

certain lean loading is a consequence of the opposite changes in the sensible and stripping terms. The sensible term increases with the lean loading, because of the higher solvent flow rate needed in the absorber to achieve 90% efficiency, which is invariant with stripper pressure. The stripping term is high at low lean loadings; because of the thorough regeneration, more stripping steam is required, but this steam does not entirely condense along the packing. The stripping heat term decreases significantly with the stripper pressure, which is in agreement with the variation predicted by the relation linking the CO_2 and H_2O partial pressures:

$$\frac{\mathrm{d}\ln P_{CO_2}}{\mathrm{d}\ln P^{sat}_{H_2O}} = \frac{-\Delta_{abs}H_{CO_2}}{\Delta_{vap}H_{H_2O}} \simeq 2 \tag{41}$$

Consequently, as the stripper pressure increases (i.e., the reboiler temperature), the ratio of partial pressure between CO_2 and H_2O increases and less stripping stream is required to desorb the same amount of CO_2.

A minimum value of 3.69 GJ/t CO_2 at 1.85 bar has been obtained by simulation for a lean loading ratio of 0.236 mol CO_2/mol MEA, which is very close to the value obtained during CASTOR tests (3.72 GJ/t CO_2 for a loading of 0.24).

The energy requirement actually decreases with stripper pressure, but it is important to notice that working at high pressure is not necessarily an optimum choice. Indeed, higher pressure certainly leads to lower heat duty but a higher-quality steam must be extracted from the power plant steam cycle, leading to an increased degradation of electrical power efficiency. For further investigations, the penalty on power plant due to steam consumption must be considered in the energy requirement, as pointed out by Le Moullec and Kanniche[2] or Liebenthal et al.,[69] in order to avoid irrelevant optimization.

6. DISCUSSIONS

Rate-based calculations involve numerous phenomena as outlined above in the section describing the mass-transfer models. Therefore, accurate estimation methods of all physical properties are mandatory to properly describe the entire process behavior in the range of operating parameters. Results obtained with the two types of mass-transfer models (enhancement factor and reaction-diffusion film) are compared in order to select the most accurate model. The aim of this part is to emphasize the role of each phenomenon in reactive separation unit by a sensitivity analysis. Lastly, the roles of H_2O and CO_2 in global heat transfer are highlighted.

6.1. Comparison between Film Models. Simulations presented in the previous sections were performed with the enhancement factor film model, which assumes a global pseudo-first-order reaction between CO_2 and MEA. The diffusion-reaction model solves the complete reaction scheme coupled with diffusion mechanisms; it requires more computational effort than the enhancement factor model but is theoretically more rigorous.

Both models have been tested in order to select the model that is most appropriate for CO_2 reactive absorption. A comparison of absorbed CO_2 fluxes between the two models is presented in Figure 10 for high and low lean loading (Runs 1A and 1E at the CASTOR pilot plant).

In both cases, the CO_2 fluxes are very similar between the two film models. The mean relative deviation is ~1% for low lean loading and ~4% for high lean loading. These deviations at

dx.doi.org/10.1021/ie302768s | Ind. Eng. Chem. Res. XXXX, XXX, XXX–XXX

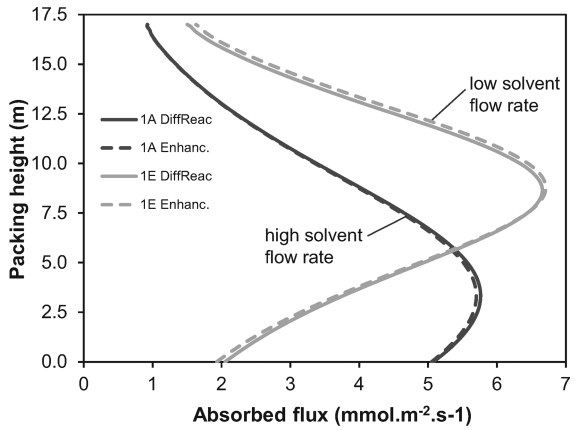

Figure 10. Comparison of CO_2 transferred flux along the absorber for the enhancement factor and diffusion-reaction models.

higher loading can be explained by the fact that less free MEA is available for a loaded solvent and, therefore, the variation of amine concentration is more pronounced along the column; the assumption of a pseudo-first-order reaction becomes more questionable.

With regard to the low differences between the two models, the use of the enhancement factor seems more appropriate in terms of computational effort, hence, its use for the simulations of reactive absorption of CO_2 in MEA. Note that this conclusion is only valid for the range of concentration, temperature, and solvent considered in this work, since the enhancement factor model is a limiting case, assuming a pseudo-first-order global reaction. For another solvent, both models must again be compared to select the one that is the most accurate, in terms of representativity, with respect to the computational effort.

6.2. Sensitivity Analysis. In order to determine the phenomenon with the greatest influence on overall performance, a nominal range sensitivity analysis is presented here. Different classes of phenomena can be identified in reactive separation columns: e.g., hydraulic properties, reactions, thermal properties, and VLE. Each of them is determined by a suitable submodel with a certain confidence range. For example, hydraulic properties (wet interfacial area and mass transfer coefficients) are typically given with a confidence range of 10%−20%.[66] Apparent reaction constants are given with ∼20% confidence.[48] VLE constants are represented with ∼25% deviation from experimental values.[33]

A simple sensitivity analysis has been performed by observing the change in the amount of CO_2 exiting the gas outlet of absorption and stripping columns when each sensitivity variable is subjected to a variation of ±10% around a nominal value. The base case corresponds to a lean loading of 0.22 with a solvent flow rate adjusted to achieve a removal efficiency of 90%. Table 3 presents the results of the sensitivity analysis for some parameters of interest.

From this simple sensitivity analysis, the limiting phenomenon for both absorption and stripping column is clearly highlighted. The absorption unit is principally driven by transfer properties, and the stripping unit is thermodynamically driven. The wet interfacial area is an important parameter, because it directly defines the total exchange area in the column and, consequently, the total absorption rate. This parameter is far more sensitive for absorption, since this operation is rate-controlled, whereas thermodynamics is the major phenomena

Table 3. Sensitivity Analysis on Main Physical Parameters: Impact of a ±10% Variation on CO_2 Exiting the Gas Outlet of Absorber and Stripper

	Sensitivity (%)			
	Absorber		Stripper	
	−10%	+10%	−10%	+10%
interfacial area	13.7	−11.4	−0.2	0.1
liquid mass-transfer coefficient	0.7	−0.6	0.1	−0.1
gas mass-transfer coefficient	9.0	−7.4	−0.3	0.3
CO_2 VLE constant	−8.7	8.3	−4.4	2.4
reaction rate	2.0	−1.7	0.1	−0.1
heat of absorption	0.3	−0.2	10.4	−11.5

to take into consideration in stripping. It appears that the choice of the thermodynamic model is crucial for a good representation of both reactive absorption and stripping (CO_2 VLE constant). As expected in this type of process, separation efficiency is not very sensitive to diffusive mass-transfer coefficients, since reactive absorption is not limited by diffusion but rather by reactions that enhance the transfer; in a nonreactive process, the influence of these coefficients would be more predominant. This point is corroborated by the influence of reaction rate on the removal efficiency, which is more important than the influence of liquid mass-transfer coefficients. Here again, variations are less important for the stripper than for the absorber. Lastly, the heat of absorption is a significant parameter for the stripping unit, since it determines the amount of CO_2 desorbed for a given amount of heat supplied. As the heat of absorption is derived from the VLE, a rigorous thermodynamic framework is once again crucial for a proper representation of limiting phenomena, especially for the stripping column.

6.3. Contributions to Heat Transfer. Modeling of chemically enhanced heat and mass transfer often focus on the determination of mass transfer but not on the different contributions to heat transfer. This part of the paper intends to give some insights on the role of CO_2, on one hand, through the heat of absorption (including enthalpy of dissolution and heat of reaction) and the role of water, on the other hand, through its evaporation and condensation.

Figure 11 represents an absorber profile of heat fluxes transferred to the liquid phase with the contribution of water and CO_2. The contribution of CO_2 is always positive due to its

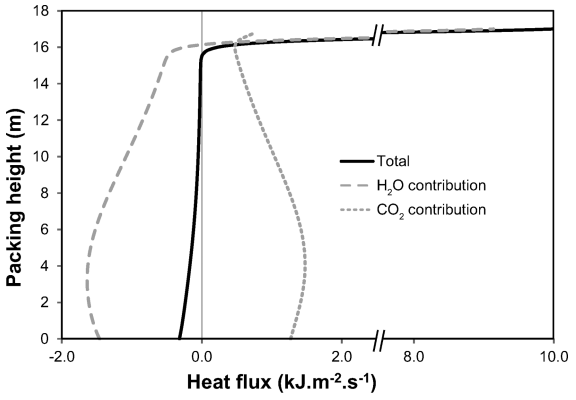

Figure 11. Total energy fluxes transferred to the liquid phase and the contribution of water condensation/evaporation and CO_2 heat of absorption along the absorber packing.

dx.doi.org/10.1021/ie302768s | Ind. Eng. Chem. Res. XXXX, XXX, XXX−XXX

constant absorption all along the packing path, reaching a maximum where the CO_2 mass transfer flux is maximum (see section 6.1). Water has a different behavior, according to the height in the absorber. As the flue gas rises in the column, water evaporates, because of the temperature increase, and therefore the thermal contribution is negative for the liquid phase. When the hot water-saturated flue gas encounters the cold lean solvent at the top of the absorber, a large amount of water condenses and releases its latent heat into the liquid phase. It explains the stiff profiles observed in Figure 11 and, consequently, the important temperature gradient observed at the top of the absorber (recall Figures 5 and 6).

Figure 12 represents the same energy fluxes for the stripping unit; the profiles are quite different, compared to the absorber.

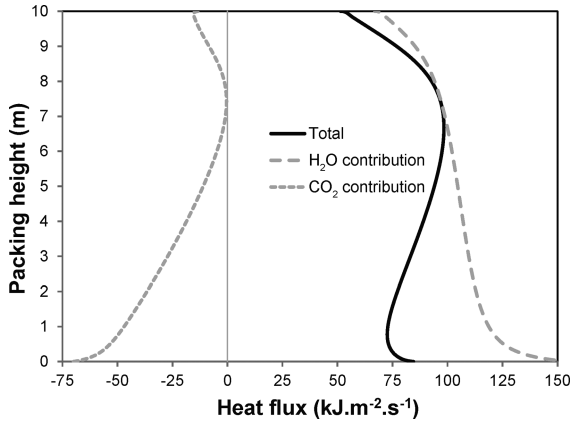

Figure 12. Total energy fluxes transferred to the liquid phase and the contribution of water condensation/evaporation and CO_2 heat of absorption along the stripper packing.

In this case, the CO_2 contribution is always negative, since the objective is to desorb this compound. The water contribution is always positive, since the thermal regeneration of the solvent is permitted by the condensation of water along the stripper packing.

Energy fluxes between phases directly impact the temperature profiles in packing, conditioning the absorption capacity in the absorber (competitive role of kinetics and thermodynamics) and regeneration capacity in the stripper (principally due to the stripping term of total reboiler heat duty). These two examples of heat flux profiles with corresponding contribution of compounds underline the major roles of CO_2 and H_2O on energy transfer for both absorption and stripping columns.

7. CONCLUSION

A rigorous rate-based column model is presented here and used for CO_2 absorption and stripping calculations. The thermodynamic representation is carried out by the extended UNIQUAC model for vapor−liquid equilibria coupled with a minimization of the total Gibbs energy for chemical equilibria in the liquid phase. A rate-based formulation of chemically enhanced heat and mass transfer is used for the modeling of a packed column with two different film models: a diffusion-reaction film and an enhancement factor model.

To validate the model, simulations are performed with an aqueous solution of 30 wt % monoethanolamine (MEA) and compared with experimental results from an industrial plant and a laboratory pilot plant. Simulation results are in excellent agreement with experimental data and the influence of lean loading ratio, stripper pressure, or solvent flow rate are correctly predicted.

The influence of the main limiting phenomena (e.g., hydrodynamics, mass transfer, thermodynamics) on the absorption performance is investigated in order to conclude the adequate degree of complexity required for this application. For the absorber, efforts should concern the characterization of gas−liquid contactors, especially for the wet interfacial area. Whatever the studied unit, phase equilibria must be carefully represented with an appropriate rigorous model such as e-UNIQUAC or e-NRTL. The two proposed film models are tested and compared. Both models give similar results; therefore, it is preferable to use the simpler one for calculation time savings. However, this conclusion is only valid for the solvent considered here, and the comparison should be done for each solvent. Insights are given on the contribution of CO_2 and H_2O on heat fluxes between phases for the absorber and the stripper. Especially, water condensation and evaporation along the packing impact directly the CO_2 removal efficiency and reboiler heat duty.

Henceforth, a state-of-the-art rate-based model is developed for the calculation of absorption and stripping columns. This generic framework allows to simulate the behavior with different solvents, using known or regressed binary interaction coefficients for the extended UNIQUAC model, as well as measurements of physicochemical properties or correlations for their calculations. The developed model is accurate, flexible, and robust enough to be coupled with an optimization algorithm and will therefore be used for parametric optimization of several flowsheet modifications and amine solvents in order to investigate their energy performances.

AUTHOR INFORMATION

Corresponding Author

*Tel.: +33 (0)3 83 17 53 90. Fax: +33 (0)3 83 32 29 75. E-mail: eric.favre@ensic.inpl-nancy.fr.

Notes

The authors declare no competing financial interest.

ACKNOWLEDGMENTS

The authors would like to acknowledge the contributors of the CASTOR project for the authorization to use results of the second testing campaign at the Esbjerg power plant. The Integrated Project CASTOR was supported by the European Commission (Contract No. SES6-CT-2004-502586).

NOMENCLATURE

a = specific area (m^2 m^{-3})
A_c = column section (m^2)
c = concentration (mol m^{-3})
C_P = heat capacity (J mol^{-1} K^{-1})
D = diffusion coefficient (m^2 s^{-1})
E = enhancement factor
G = molar gas flux (mol s^{-1})
h = heat-transfer coefficient (W m^{-2} K^{-1})
$\overline{H_i}$ = partial molar enthalpy (J mol^{-1})
H_C = column height (m)
Ha = Hatta number
$\mathcal{H}$ = Henry's constant (Pa)
J = diffusive flux (mol m^{-2} s^{-1})
k = mass-transfer coefficient (m s^{-1})
K = reaction or VLE constant

L = molar liquid flux (mol s^{-1})
N = molar flux (mol m^{-2} s^{-1})
N_C = total number of compounds
N_G = number of gas species
N_R = number of reactions
P = pressure (Pa)
q = heat flux (W m^{-2})
r = reaction rate (mol m^{-3} s^{-1})
$\mathcal{R}_i$ = production rate by reactions (mol m^{-3} s^{-1})
R = ideal gas constant (J mol^{-1} K^{-1})
t = time (s)
T = temperature (K)
v = molar volume (m^3 mol^{-1})
x = liquid mole fraction
y = gas mole fraction
z = axial coordinate

Greek Letters

α = loading (mol CO_2 mol MEA^{-1})
δ = film thickness (m)
γ = activity coefficient
μ = chemical potential (J mol^{-1})
ν = stoichiometry coefficient
φ = fugacity coefficient
ξ = coordinate in film (m)

Superscripts

∞ = infinite dilution or instantaneous reaction
0 = reference
B = bulk
G = gas
I = interfacial
in = input
L = liquid
sat = saturation
VLE = vapor−liquid equilibria

Subscripts

eff = effective
i = compound
L = lean
ov = overall
R = rich
tot = total

Acronyms

AARD = average absolute relative deviation (%)
CFD = computational fluid dynamics
DEA = diethanolamine
MEA = monoethanolamine
MDEA = methyl-diethanolamine
PZ = piperazine
SAFT = Statistical Associating Fluid Theory

REFERENCES

(1) International Energy Agency. *World Energy Outlook*, 2011; http://www.iea.org/weo/.

(2) Le Moullec, Y.; Kanniche, M. Screening of flowsheet modifications for an efficient monoethanolamine (MEA) based post-combustion CO_2 capture. *Int. J. Greenhouse Gas Control* **2011**, *5*, 727−740.

(3) Ma'mun, S.; Svendsen, H. F.; Hoff, K. A.; Juliussen, O. Selection of new absorbents for carbon dioxide capture. *Energy Convers. Manage.* **2007**, *48*, 251−258.

(4) Puxty, G.; Rowland, R.; Allport, A.; Yang, Q.; Bown, M.; Burns, R.; Maeder, M.; Attalla, M. Carbon Dioxide Postcombustion Capture: A Novel Screening Study of the Carbon Dioxide Absorption Performance of 76 Amines. *Environ. Sci. Technol.* **2009**, *43*, 6427−6433.

(5) Cousins, A.; Wardhaugh, L.; Feron, P. H. M. A Survey of process flow sheet modifications for energy efficient CO_2 capture from flue gases using chemical absorption. *Int. J. Greenhouse Gas Control* **2011**, *5*, 605−619.

(6) Amrollahi, Z.; Ystad, P.; Ertesvag, I.; Bolland, O. Optimized process configurations of post-combustion CO_2 capture for natural-gas-fired power plant—Power plant efficiency analysis. *Int. J. Greenhouse Gas Control* **2011**, *8*, 1−11.

(7) Pacheco, M. *Mass Transfer, Kinetics and Rate-Based Modeling of Reactive Absorption*. Ph.D. Thesis, The University of Texas, Austin, TX, 1998.

(8) deMontigny, D.; Aboudheir, A.; Tontiwachwuthikul, P. Modelling the performance of a CO_2 absorber containing structured packing. *Ind. Eng. Chem. Res.* **2006**, *45*, 2594−2600.

(9) Gabrielsen, J.; Michel, M.; Stenby, E.; Kontogeorgis, G. Modeling of CO_2 absorber using an AMP Solution. *AIChE J.* **2006**, *52*, 3443−3451.

(10) Tobiesen, F.; Svendsen, H.; Juliussen, O. Experimental validation of a rigorous absorber model for CO_2 postcombustion capture. *AIChE J.* **2007**, *53*, 846−863.

(11) Lawal, A.; Wang, M.; Stephenson, P.; Yeung, H. Dynamic modelling of CO_2 absorption for post combustion capture in coal-fired power plants. *Fuel* **2009**, *88*, 2455−2462.

(12) Huepen, B.; Kenig, E. Rigorous Modeling and Simulation of an Absorption-Stripping Loop for the Removal of Acid Gases. *Ind. Eng. Chem. Res.* **2010**, *49*, 772−779.

(13) Gaspar, J.; Cormos, A.-M. Dynamic modeling and validation of absorber and desorber columns for post-combustion CO_2 capture. *Comput. Chem. Eng.* **2011**, *35*, 2044−2052.

(14) Khan, F.; Krishnamoorthi, V.; Mahmud, T. Modelling reactive absorption of CO_2 in packed columns for post-combustion carbon capture applications. *Chem. Eng. Res. Des.* **2011**, *89*, 1600−1608.

(15) Dugas, R.; Alix, P.; Lemaire, E.; Broutin, P.; Rochelle, G. Absorber model for CO_2 capture by monoethanolamine—Application to CASTOR pilot results. *Energy Procedia* **2009**, *1*, 103−107.

(16) Tobiesen, F.; Svendsen, H.; Juliussen, O. Experimental validation of a rigorous desorber model for CO_2 post-combustion capture. *Chem. Eng. Sci.* **2008**, *63*, 2641−2656.

(17) Kent, R.; Eisenberg, B. Better data for amine treating. *Hydrocarbon Process.* **1976**, *55*, 87−90.

(18) Furst, W.; Renon, H. Representation of excess properties of electrolyte solutions using a new equation of state. *AIChE J.* **1993**, *39* (2), 335−343.

(19) Vallée, G.; Mougin, P.; Jullian, S.; Fürst, W. Representation of CO_2 and H_2S absorption by aqueous solutions of diethanolamine using an electrolyte equation of state. *Ind. Eng. Chem. Res.* **1999**, *38*, 3473−3480.

(20) Button, J.; Gubbins, K. SAFT prediction of vapour−liquid equilibria of mixtures containing carbon dioxide and aqueous monoethanolamine or diethanolamine. *Fluid Phase Equilib.* **1999**, *158−160*, 175−181.

(21) Deshmukh, R.; Mather, A. E. A Mathematical Model for Equilibrium Solubility of Hydrogen Sulfide and Carbon Dioxide in Aqueous Alkanolamine Solutions. *Chem. Eng. Sci.* **1981**, *36*, 355−362.

(22) Weiland, R.; Chakravarty, T.; Mather, A. Solubility of Carbon Dioxide and Hydrogen Sulfide in Aqueous Alkanolamines. *Ind. Eng. Chem. Res.* **1993**, *32*, 1419−1430.

(23) Pitzer, K. Theoretical Basis and General Equations. *J. Phys. Chem.* **1973**, *77* (2), 268−277.

(24) Böttinger, W.; Maiwald, M.; Hasse, H. Online NMR Spectroscopic Study of Species Distribution in MDEA−H_2O−CO_2 and MDEA−PIP−H_2O−CO_2. *Ind. Eng. Chem. Res.* **2008**, *47*, 7917−7926.

(25) Chen, C.-C. A local composition model for the excess Gibbs energy of aqueous electrolyte systems. I: Single completely dissociated electrolyte single solvent systems. *AIChE J.* **1982**, *28*, 588−596.

(26) Chen, C.; Evans, L. A local composition model for the excess Gibbs energy of aqueous electrolyte systems. *AIChE J.* **1986**, *32*, 444−454.
(27) Austgen, D.; Rochelle, G.; Peng, X.; Chen, C.-C. Model of Vapor−Liquid Equilibria for Aqueous Acid Gas−Alkanolamine Systems Using the Electrolyte−NRTL Equation. *Ind. Eng. Chem. Res.* **1989**, *28*, 1060−1073.
(28) Posey, M. *Thermodynamic Model for Acid Gas Loaded Aqueous Alkanolamine Solutions*. Ph.D. Thesis, The University of Texas, Austin, TX, 1996.
(29) Hessen, E.; Haug-Warberg, T.; Svendsen, H. The refined e-NRTL model applied to CO_2−H_2O alkanolamine systems. *Chem. Eng. Sci.* **2010**, *65*, 3638−3648.
(30) Sander, B. *Extended UNIFAC/UNIQUAC Models for (1) Gas Solubilities and (2) Electrolyte Solutions*. Ph.D. Thesis, Technical University of Denmark, Lyngby, Denmark, 1984.
(31) Thomsen, K.; Rasmussen, P. Modeling of vapor−liquid−solid equilibrium in gas−aqueous electrolyte systems. *Chem. Eng. Sci.* **1999**, *54*, 1787−1802.
(32) Faramarzi, L.; Kontogeorgis, G.; Thomsen, K.; Stenby, E. Extended UNIQUAC model for thermodynamic modeling of CO_2 absorption in aqueous alkanolamine solutions. *Fluid Phase Equilib.* **2009**, *282*, 121−132.
(33) Aronu, U.; Gondal, S.; Hessen, E.; Haug-Warberg, T.; Hartono, A.; Hoff, K.; Svendsen, H. Solubility of CO_2 in 15, 30, 45 and 60 mass % MEA from 40 to 120 °C and model representation using the extended UNIQUAC framework. *Chem. Eng. Sci.* **2011**, *24*, 6393−6406.
(34) Abrams, D.; Prausnitz, J. Statistical thermodynamics of liquid mixtures: A new expression for the excess Gibbs energy of partly or completely miscible system. *AIChE J.* **1975**, *21* (1), 116−128.
(35) Guggenheim, E. A. *Mixtures: The Theory of the Equilibrium Properties of Some Simple Classes of Mixtures, Solutions and Alloys*; Clarendon Press: Oxford, U.K., 1952.
(36) Smith, W.; Missen, R. *Chemical Reaction Equilibrium Analysis: Theory and Algorithms*, Second Edition; Wiley: New York, 1982.
(37) Austgen, D. *A Model for Vapor−Liquid Equilibria for Acid Gas−Alkanolamine−Water Systems*. Ph.D. Thesis, The University of Texas, Austin, TX, 1989.
(38) Greiner, H. An effecient implementation of Newton's method for complex nonideal chemical equilibria. *Comput. Chem. Eng.* **1991**, *15*, 115−123.
(39) Michelsen, M.; Mollerup, J. *Thermodynamics Models: Fundamentals and Computational Aspects*, Second Edition; Tie-Line Publications: Holte, Denmark, 2007.
(40) Noeres, C.; Kenig, E.; Gòrak, A. Modelling of reactive separation processes: reactive absorption and reactive distillation. *Chem. Eng. Process.* **2003**, *42*, 157−178.
(41) Kenig, E.; Schneider, R.; Gorak, A. Reactive absorption: Optimal process design via optimal modelling. *Chem. Eng. Sci.* **2001**, *56* (2), 343−350.
(42) Higler, A.; Krishna, R.; Taylor, R. Nonequilibrium cell model for multicomponent (reactive) separation processes. *AIChE J.* **1999**, *45*, 2357−2370.
(43) Yin, F.; Sun, C.; Afacan, A.; Nandakumar, K.; Chuang, K. CFD Modeling of Mass-Transfer Processes in Randomly Packed Distillation Columns. *Ind. Eng. Chem. Res.* **2000**, *39*, 1369−1380.
(44) Taylor, R.; Krishna, R. *Multicomponent Mass Transfer*; John Wiley & Sons: New York, 1993.
(45) Benjelloun-Dabagh, Z.; Cadours, R.; Cauvin, S.; Mougin, P. A New Approach for Chemical Transfer Reaction Models. *Comput.-Aided Chem. Eng.* **2008**, *25*, 641−646.
(46) Kucka, L.; Müller, I.; Kenig, E.; Gorak, A. On the modelling and simulation of sour gas absorption by aqueous amine solutions. *Chem. Eng. Sci.* **2003**, *58*, 3571−3578.
(47) Krishna, R.; van Baten, J. In silico screening of zeolite membranes for CO_2 capture. *J. Membr. Sci.* **2010**, *360*, 323−333.
(48) Aboudheir, A.; Tontiwachwuthikul, P.; Chakma, A.; Idem, R. Kinetics of the reactive absorption of carbon dioxide in high CO_2-loaded, concentrated aqueous monoethanolamine solutions. *Chem. Eng. Sci.* **2003**, *58*, 5195−5210.
(49) Puxty, G.; Rowland, R. Modeling CO_2 Mass Transfer in Amine Mixtures: PZ-AMP and PZ-MDEA. *Environ. Sci. Technol.* **2011**, *45*, 2398−2405.
(50) Bird, R.; Stewart, W.; Lightfoot, E. *Transport Phenomena*, Revised, Second Edition; John Wiley & Sons: New York, 2006.
(51) Finlayson, B. *Nonlinear Analysis in Chemical Engineering*; McGraw−Hill: New York, 1980.
(52) More, J.; Garbow, B.; Hillstrom, K. *User Guide for MINPACK-1*. Technical Report No. ANL-80-74, Argonne National Laboratory, Argonne, IL, 1980.
(53) DeCoursey, W. Enhancement factors for gas absorption with reversible reaction. *Chem. Eng. Sci.* **1982**, *37*, 1483.
(54) Chang, C.-S.; Rochelle, G. Mass Transfer Enhanced by Equilibrium Reactions. *Ind. Eng. Chem. Fundam.* **1982**, *21*, 378−385.
(55) Olander, D. Simultaneous mass transfer and equilibrium chemical reaction. *AIChE J.* **1960**, *6*, 233−239.
(56) Luo, X.; Knudsen, J.; de Montigny, D.; Sanpasertparnich, T.; Idem, R.; D., G.; Notz, R.; Hoch, S.; Hasse, H.; Lemaire, E.; Alix, P.; Tobiesen, F.; Juliussen, O.; Köpcke, M.; Svendsen, H. Comparison and validation of simulation codes against sixteen sets of data from four different pilot plants. *Energy Procedia* **2009**, *1*, 1249−1256.
(57) Weiland, R.; Dingman, J.; Cronin, D.; Browning, G. Density and viscosity of some partially carbonated aqueous alkanolamine solutions and their blends. *J. Chem. Eng. Data* **1998**, *43*, 378−382.
(58) Wilke, C. A viscosity equation for gas mixtures. *J. Chem. Phys.* **1950**, *18*, 517−554.
(59) Peng, D.-Y.; Robinson, D. A new two-constant equation of state. *Ind. Eng. Chem. Fundam.* **1976**, *15*, 59−64.
(60) Vazquez, G.; Alvarez, E.; Navaza, J.; Rendo, R.; Romero, E. Surface tension of binary mixtures of water + monoethanolamine and water + 2-amino-2-methyl-1-propanol and tertiary mixtures of these amines with water from 25 °C to 50 °C. *J. Chem. Eng. Data* **1997**, *42*, 57−59.
(61) Fuller, E.; Ensley, K.; Giddings, J. A new method for prediction of binary gas-phase diffusion coefficients. *Ind. Eng. Chem.* **1966**, *58*, 18−27.
(62) Wilke, C.; Chang, P. Correlation of diffusion coefficients in dilute solutions. *AIChE J.* **1955**, *1*, 264−270.
(63) Horvath, A. *Handbook of Aqueous Electrolyte Solutions*; Ellis Horwood, Ltd.: Chichester, U.K., 1985.
(64) Hilliard, M. *A Predictive Thermodynamic Model for an Aqueous Blend of Potassium Carbonate, Piperazine, and Monoethanolamine for Carbon Dioxide Capture from Flue Gas*. Ph.D. Thesis, The University of Austin, Austin, TX, 2008.
(65) Poling, B.; Prausnitz, J.; O'Connel, J. *The Properties of Gases and Liquids*, Fifth Edition; McGraw−Hill: New York, 2001.
(66) Hanley, B.; Chen, C.-C. New mass-transfer correlations for packed towers. *AIChE J.* **2012**, *58*, 132−152.
(67) Kim, I.; Svendsen, H. Heat of absorption of carbon dioxide (CO_2) in monoethanolamine (MEA) and 2-(aminoethyl) ethanolamine (AEEA) solutions. *Ind. Eng. Chem. Res.* **2007**, *46*, 5803−5809.
(68) Le Bouhelec, E.; Mougin, P.; Barrea, A.; Solimando, R. Rigorous Modeling of the Acid Gas Heat of Absorption in Alkanolamine Solutions. *Energy Fuels* **2007**, *21*, 2044−2055.
(69) Liebenthal, U.; Linnenberg, S.; Oexmann, J.; Kather, A. Derivation of correlations to evaluate the impact of retrofitted post-combustion CO_2 capture processes on steam power plant performance. *Int. J. Greenhouse Gas Control* **2011**, *5*, 1232−1239.